M. R. Radio

S. A. Schmitt

S. H. Lewis

T. G. Merry

J. L. Evjen

Precision Automatic Measuring of X-Y Coordinates

Abstract: This paper reports the development of a computer-controlled machine for non-contact inspection of manufactured parts. The machine, called PAMM (Precision Automatic Measuring Machine), is capable of providing "on-the-fly" measurements accurate to within 100 microinches. The intersection of a rotating spiral slot with a stationary linear slot produces a moving aperture for scanning in small increments over a projected, enlarged image of a part. The scanner assembly moves along an overhead cantilever beam in the x direction, and the part being inspected moves in the y direction along the machine base; position in each direction is monitored by a separate laser interferometer.

In the paper conventional methods of coordinate measuring are briefly reviewed, the details of the new design are presented, some experimentally obtained measurements are given, measurement errors induced by photodetector shot noise and aperture roughness are analyzed, and the computer-control and data-analysis techniques are discussed.

Introduction

Many of today's mechanical assemblies call for a diversity of precisely specified component parts that must be manufactured with extreme accuracy. The trend is toward reduction in dimensional tolerances and in the amount of part deformation that will be permitted in the operating environment of the part.

The demand for highly accurate manufacturing brings with it the need for improvements in the methods used to inspect the dimensions of finished parts. Conventional inspection techniques are often time-consuming and can result in considerable amounts of lost machine-tool time simply because of the delay in reporting inspection results. When high-precision measurements are needed, the inspection problem is compounded. Some of the difficulties in using conventional methods for precise measuring are the following:

- 1) Distances between surfaces checked by a probing indicator are normally point-to-point rather than surface-to-surface measurements; surface variations become significant as tolerances decrease.
- 2) When the tolerances being checked are very small, it is difficult for two inspectors to agree. Identical readings between two gauges made to the same specification are likewise difficult to attain.
- 3) Frequently the machine operator and the inspector use different measuring methods.

- 4) When very precise measuring equipment is being used the inspectors must be specially trained in the use and maintenance of such equipment.
- 5) Pressures on the inspector are great when precise parts are urgently needed; these pressures cause tension and error.
- 6) Data must be handwritten.
- 7) Continuing records of tolerance control are difficult to maintain. Requests for reducing allowable tolerances require extensive feasibility studies.

Previous work on the measurement problem has included upgrading of microscopes and comparators with improvements in optics, linear measuring devices and lamps. Electronic differential gauges have reduced the time needed for inspection of holes and dots that can be mechanically probed. Coordinate-measuring machines have reduced set-up time and inspection time for certain applications. Machine tools have been improved for closer tolerance capabilities. More accurate tooling and machining techniques have helped to improve tolerance control. However, more complex part configurations, reduced size, and closer tolerances are constantly testing the state-of-the-art in measurement requirements and have created the need for a precision automatic measuring machine.

The purpose of the work reported in this paper is to overcome the difficulties listed above. A solution is given by a device called the Precision Automated Measuring Machine (PAMM). The main design considerations for

The authors are located at the IBM General Systems Division plant in Rochester, Minnesota. 55901

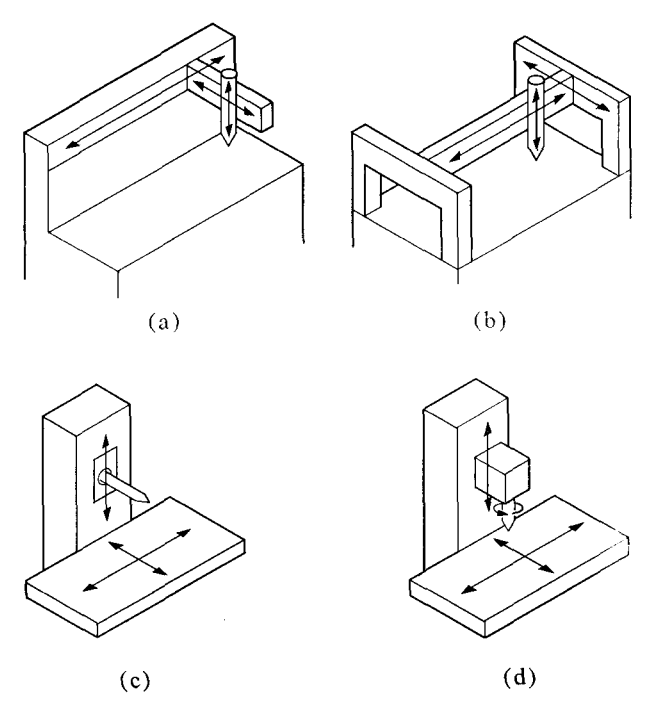


Figure 1 Coordinate measuring machines. (a) Cantilever CMM is easily accessible for loading and unloading and for getting at faces of a cube; (b) bridge CMM is more rigid than cantilever and is less subject to inaccuracies due to deflection; (c) horizontal boring machine is used to inspect parts such as gear boxes which have "through" holes; (d) vertical jig boring machine is sometimes called "universal machine" because of its versatility.

this machine and the selected design approaches are presented in the next section of the paper. Other sections give the results of studies performed to validate the design, some analytical work on the sources of measurement error, and an explanation of how a computer system is being used to control PAMM operation.

Design considerations

The device considered in this paper is a type of instrument called a coordinate measuring machine (CMM). CMM's are used to measure the geometrical features of machine parts in terms of their locations in a two-dimensional Cartesian-coordinate system. A general characteristic of any CMM is that it contains a table on which the part to be measured is placed and has some inspection tool for identifying the point on the part where the coordinates are to be measured.

In designing a CMM to satisfy a particular set of requirements the following considerations are of major importance:

- 1) What kind of inspection tool is to be used?
- 2) How is the machine base to be structured to guide the motions of the part table and/or the inspection tool?

3) What kind of measurement scheme will be used to monitor the position of the table and the inspection tool?

The main requirements for the proposed Precision Automated Measuring Machine are that measurement accuracy should be ± 0.0001 . in. and that the measurement surface of the part should be scanned at a rate of about 0.5 in./sec.

• Scanner

A common type of inspection tool is a conical probe whose tip touches the part at the selected measuring place. The use of a probe, however, severely limits the speed with which a part can be thoroughly inspected. The requirement for high-speed measuring meant that some kind of noncontact inspection tool was necessary. This observation led to an examination of various optical scanning techniques. It was determined that a cathoderay-tube flying-spot scanner, such as those used in optical character recognition systems, could not produce a small enough spot nor could it provide sufficient consistency in spot size at various points on the tube face to yield the desired accuracy. Other experiments were conducted to determine the merits of single-spot laser scanning. Although small enough spots could be obtained, this scheme was judged impractical because it required too frequent and rapid motion of the part table.

The design of a suitable optical scanning method is the main contribution reported in this paper. In this method a magnified image of the part being measured is projected onto the surface of a revolving disk which contains a transparent spiral slot and a number of equally spaced transparent "timing slots" around its edge. Light passing through the spiral impinges on a stationary plate that contains a transparent slot oriented radially to the axis of the disk. The combination of the revolving spiral slot and the stationary linear slot produces a moving aperture that permits a small area of the projected part to be inspected. A photodetector circuit receives the light transmitted through the aperture and converts it to an electrical signal. Light transmitted through the timing slots causes pulses to be generated for the purpose of monitoring the aperture position during a scan. The characteristics of the scanner are discussed in detail in later sections.

• Machine base

Some typical arrangements of structural elements found in commercially available CMM's¹ are illustrated in Fig. 1. The choice of a particular method for guiding inspectiontool and part-table motion depends to a considerable extent on whether the structure is rigid enough to yield the required measurement accuracy. The machine base chosen for the PAMM is shown schematically in Fig. 2.

It contains a table which moves the part to be measured in the y direction and an overhead granite bridge on which a granite carriage floats on an air-bearing film. The scanning system, which weighs about 100 lbs., is transported in the x direction by the carriage. The suitability of this machine base for use in the PAMM was determined by an experimental analysis. A later section of the paper reports the effects of applying various loads and torques at critical points on the carriage.

• Position monitoring

Four techniques for accurately measuring the positions of the part table and scanner carriage with respect to a reference line were considered. One technique, exemplified by the DIG Fine Encoder system, involves optical reading of a precisely ruled scale. Another technique, as used in the Inductosyn system, employs two sets of equally spaced inductors mounted on surfaces which move with respect to each other. When one set of coils is excited by an oscillating signal, the signal induced in the other set varies periodically with the amount of coupling between the two sets of coils. Distance is measured by counting the number of times maximum and minimum coupling occurs during coil movement. A third method makes use of the Moiré fringe pattern produced as a precisely ruled linear grating is rotated with respect to another one. 4,5

The fourth method considered is a laser interferometer system in which distances are measured in units of one-half wavelengths of a He-Ne laser. In an atmosphere containing 0.03% CO₂ at 20°C and 706 Torr, the half-wave-lengths are 0.000012460460 in. This type of system was judged to provide the best combination of accuracy, stability and control characteristics for the proposed application. The Appendix to this paper shows how a system employing a laser beam and two standard Michelson interferometers is used to measure distances in the x and y directions.

Design validation

In choosing a specific design for the optical scanner trade-offs had to be made among the important parameters: magnification, aperture area and disk rpm, in order to achieve acceptable values of scan rate, resolution and error. The following considerations indicate how the parameters affect performance:

- 1) A reduction in aperture area increases resolution, but it also increases error due to noise in the photodetector signal until, at some point, the signal noise limits the resolution.
- 2) An increase in the magnification increases the resolution, but reduces the scan rate and the length of scan. It does not affect the signal noise error, but it does reduce error due to slot-edge roughness.

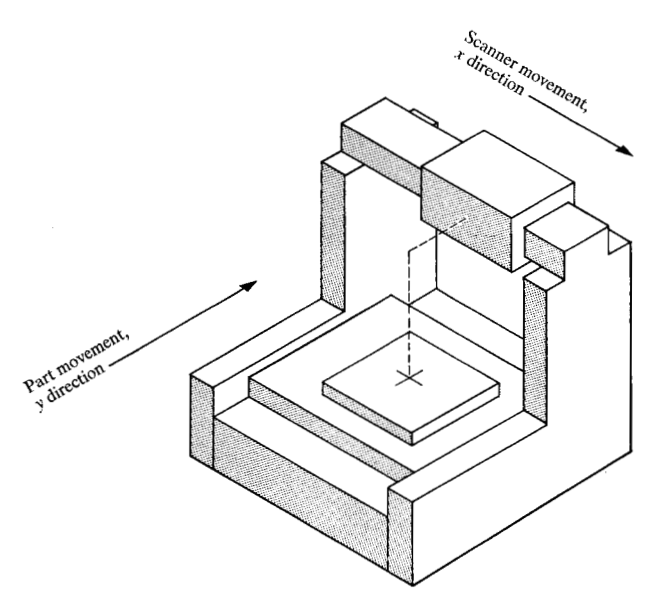


Figure 2 Geometry of base for measuring machine.

3) An increase in the disk rpm increases signal noise error, but does not affect resolution and length of scan.

Other variables that affect results are the choices of photodetectors, light source and aperture shape. Both a more intense light source and a more sensitive detector increase photodetector current and thereby reduce noise error. The intensity of a thermal light source varies approximately with the fourth power of its absolute temperature. Also, the wavelength of the source light becomes shorter as the temperature increases. These facts make it important to use a very hot light source. However, the source must also have a uniform intensity if the detector circuits are to operate properly.

• Feasibility studies of scanner

To test the feasibility of the design approach an experimental scanner carriage was built (Fig. 3). The carriage permitted the scanner to travel a distance of 4.5 in. During the feasibility study no effort was made to incorporate an interferometer system to monitor x-y travel.

The scanning disk itself was made of optical glass coated on one side with an opaque emulsion. Part of the emulsion was removed to produce a 0.005-in. wide spiral pattern. The spiral radius decreased at a constant rate over 360° from a maximum of 4.5 in. to a minimum of 1.5 in.

The stationary plate placed behind the disk was also coated with an opaque emulsion partially removed to form a 0.005-in. wide linear slot. The rate of aperture motion in inches per second as the disk revolves can be calculated from the expression r = ls/M, where l is the

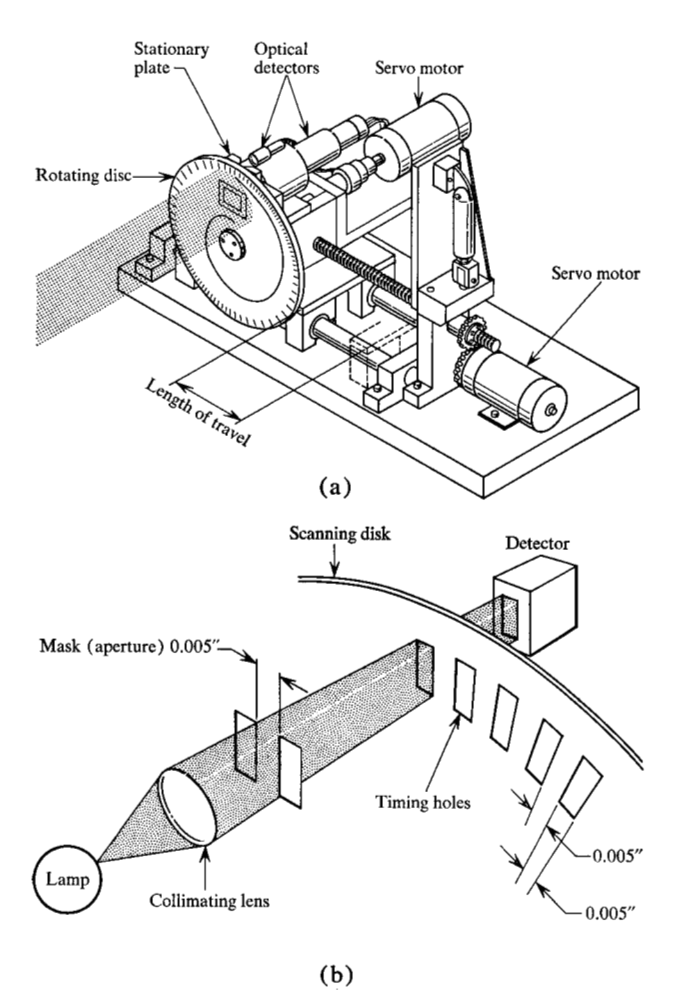


Figure 3 (a) Scanner arrangement for precision automated measuring machine. (b) detail of timing slots.

difference in inches between the maximum and minimum radii of the spiral, s is rotational speed of the disk in revolutions per second and M is the magnification of the projected image of the part.

The experimental disk had 600 timing holes equally spaced around its edge. The scanner was operated at 1000 rpm and the part image was projected at 10×1000 magnification. These parameter values yielded 600×1000 (100) = 10,000 timing pulses per second and 600×100 (10/3in.) = 2000 pulses per inch of scan.

To make a measurement, the edge of the part must be detected and correlated with the timing pulses. The photodetector output has the maximum value I when the aperture is fully illuminated and goes linearly to zero when the aperture is not illuminated. When the aperture is centered over the edge of a part, the detector output is approximately I/2. The accuracy of the measurement is determined by how close the I/2 point can be detected and correlated to the timing pulses. The error in any

measurement will be the sum of the error due to photodetector signal noise and the error due to the spacing of the timing holes.

The experimental device was used to measure four different parts: 1) the height of a rectangular hole in an 80-hole carbide punch plate, 2) a 0.0057-in. diameter hole in a brass plate, 3) a 0.00078-in. diameter brass wire and 4) a 0.0004-in. diameter tungsten wire. After each scan, the part was moved manually to enable a new area to be scanned.

Hole size measurements on the 80-hole plate were made by using a high-speed counter to count the timing pulses. The count was regularly either 501 or 502 counts per scan. Since each count corresponds to 0.00025 in., the measurements ranged from 0.12525 to 0.12550 in., a variation of 0.00025 in. For purposes of comparison, a measurement was made with electronic differential probes. The result was a measurement of 0.12528 in.

The pulse count for the 0.0057-in. diameter hole was 23, or, converted to inches, 0.00575 in. This differed by 50 microinches from a microscope measurement.

The counter was not used to measure the two wires. Instead, the photodetector output was displayed on an oscilloscope. Figures 4(a) and 4(b) show the results for the 0.0004-in. and 0.0008-in. wires, respectively. With a horizontal scale of 0.2 msec or 0.001-in. per division, the oscilloscope traces give measurements of 0.00043-in. and 0.00090 in., respectively. These results were reproducible within 50 microinches. Figure 4(c) shows the photodetector output when light intensity was reduced, indicating the effect of detector shot-noise on the output.

The scanning system was altered to increase the accuracy of the measurements. A lens system utilizing three standard objectives was installed. The magnifications are $5 \times ,10 \times$, and $20 \times$. A new disk was made; it has 3000 timing slots, which makes it possible to break the 3-in. scanning line into 3000 increments, each 0.001 in. long.

It is possible by electronic means to double or quadruple the number of timing pulses, thus providing smaller increments along a scanning line. A full-wave rectifier circuit is used to double the pulse frequency. Since the input to the rectifier is a triangular wave, the output is also triangular, thus making it possible to double the pulse frequency as many times as desired.

The widths of the spiral slot and the stationary slot were retained at 0.005 in. since this dimension provides a good compromise between accuracy and resolution.

• Edge detection circuit

The performance of the measuring machine depends in part on how well the photodetector signal can be analyzed to find its half-amplitude point. Since the signal is a ramp function, generating its second derivative would provide a convenient means of detecting the edge: the second derivative of a descending ramp changes from positive to negative at the midpoint of the ramp. However, in differentiating the signal twice it is quite possible to obtain a signal-to-noise ratio of unity. For example, if T is the time required for an aperture to cross the edge of a part, the amplitude of the second derivative of a ramp of height I is on the order of I/T^2 . A noise pulse with a rise time of T/10 and an amplitude of I/100 will also yield a second derivative with an amplitude of approximately I/T^2 :

$$\frac{\Delta}{\Delta T} \frac{\Delta I}{\Delta T} = \left(\frac{1}{T/10}\right) \left(\frac{I/100}{T/10}\right) = \frac{I}{T^2}.$$

Since the convenience of using differentiating circuits is outweighed by their sensitivity to noise, a circuit was designed to analyze directly the photodetector output. The circuit was designed to be highly insensitive to noise, to compensate for variations in the signal level and also to accommodate signals where the "dark level" is not zero, such as occurs when measurements are made with light reflected from the part. Figure 5 shows a schematic diagram of the circuit.

The signal from the photodetector is preamplified and fed into four circuits. The first circuit is a diode clamp circuit which determines the approximate upper level of the waveform. Two voltage dividers at the output of this circuit produce dc voltages of approximately V/4 and 3V/4 where V is the magnitude of the upper voltage.

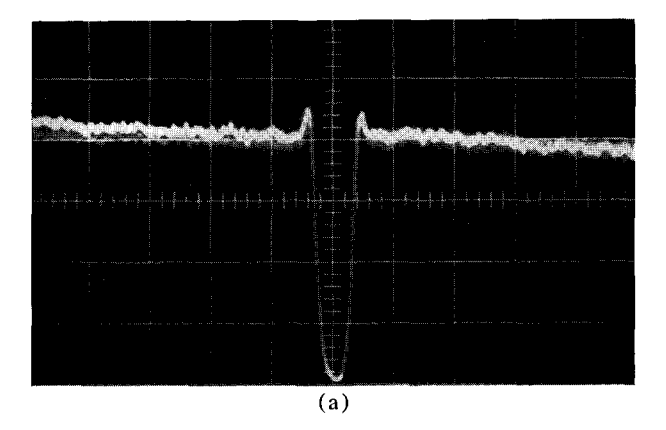
The next two circuits in the system find the average upper and lower voltage levels of input signal and also hold these voltages. When input level exceeds 3V/4, Comparator 2 is turned on. This turns on an electronic switch which passes the signal from the preamplifier to a low-pass filter and hold circuit that finds the average upper level of the waveform. When the input waveform falls below 3V/4 the comparator turns off and the upper voltage level is held.

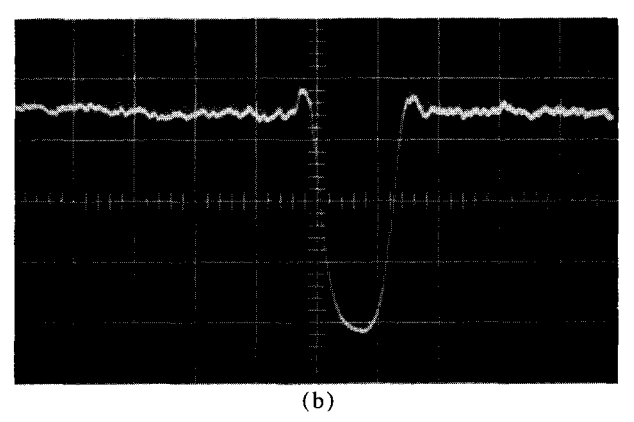
Comparator 1 is turned on when the input level falls below V/4. This allows the average lower level to be found and held by the low-pass filter 1. The voltage divider at the outputs of the hold circuits 1 and 2 produces a voltage V/2 which is compared to the input waveform by Comparator 3. Figure 6(a) shows the input waveform produced from a reflective surface with dark bands on it. Also shown is the output from the squaring circuit. Figure 6(b) shows expanded view of one dark band.

Machine base study

The PAMM design required the chosen base (Fig. 2) to perform under unique conditions for which no existing experimental data was available. Consequently, tests were performed to obtain sufficient confidence in the base.

Since the carriage is suspended on an air film between itself and the bridge, it is subject to yaw, pitch and roll.





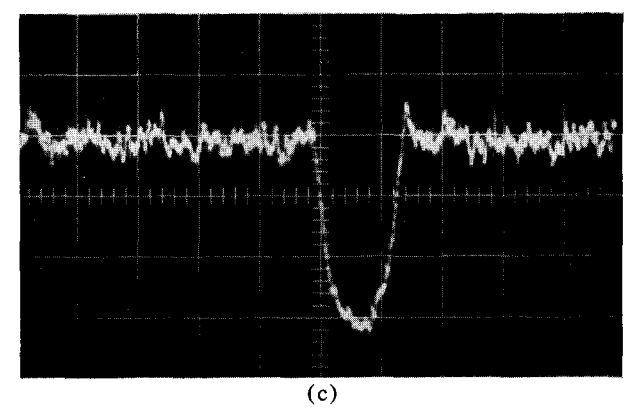


Figure 4 Oscillograms of photodetector output obtained during feasibility experiments with scanning concept. (a) 0.0004-in. diameter wire; (b) 0.0008-in. diameter wire (c) 0.0008-in. diameter wire; reduced light intensity increases noise.

The air-bearing design is intended to give a resisting effect when such conditions exist, but some deflections must occur before this resisting effect can take place.

Note the four load forces applied to produce the deflections as illustrated in Fig. 7. Load force 1 tested the ability of the carriage to carry various weights. The results of this test [Fig. 8 (a)] indicate that the carriage will carry the 100 pound scanner with at least 150 microinches of air film when 30 psi or higher air pressure is

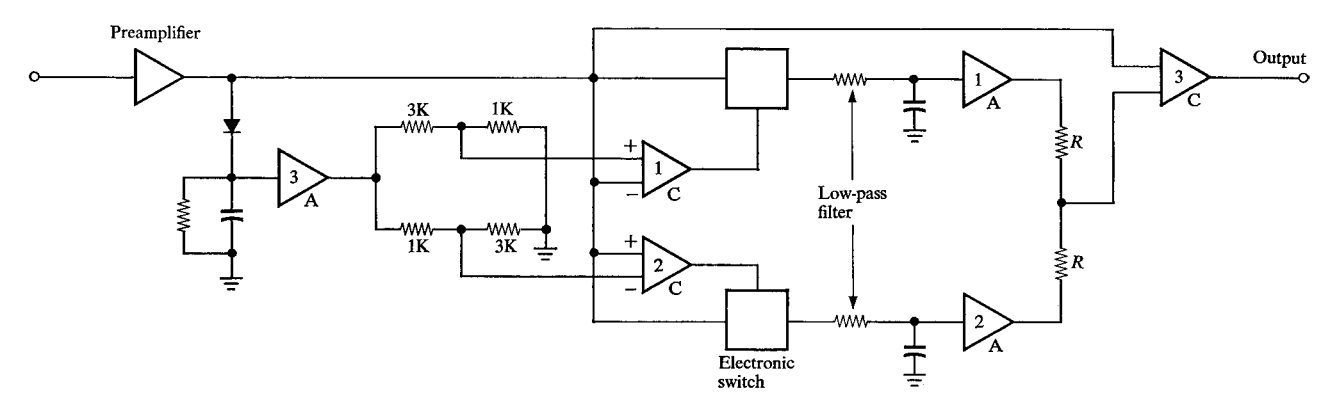
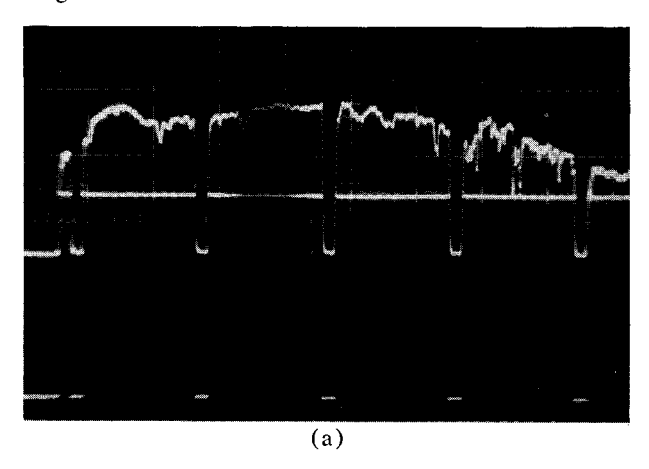
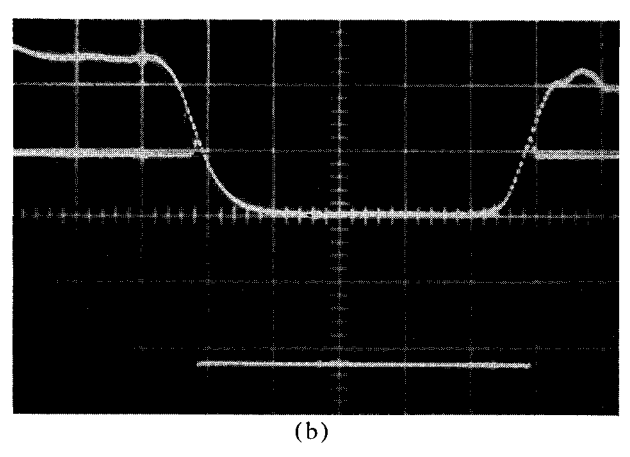


Figure 5 Schematic diagram of edge detector circuit.

Figure 6 Input signal to edge detector circuit. (a) Signal resulting from scanning a reflecting surface with dark bands; (b) expanded view of signal corresponding to a single dark band.





supplied. Load forces 2 and 3 produced deflections in the measurement point up to 0.0005 inches when the torque reached 10 foot pounds. This deflection would be present if the bridge were not properly balanced. It would be constant, however, and would not introduce a measurement error if the air pressure remained constant. The bridge would, of course, be balanced as well as possible.

The load force 4 indicated in Fig. 7 simulates the torque applied under the PAMM operational conditions. Maximum design acceleration is 0.125 in./sec². This requires a force of 0.76 lb. to accelerate the carriage and scanner. The bridge and carriage construction make it impractical to drive the carriage at its center of mass. Thus, the force is applied several inches from center. Fig. 8(b) illustrates the deflections that occur when various amounts of torque are applied. Note that in the range of the PAMM application, the error will be less than 10 microinches.

Another test was performed in which vibration at the measurement point was observed while the scanner was rotated at 2,100 rpm. Several resonant points were noted at low rpm, but the vibration increase due to the spindle rotation at the design speed was not detectable. External vibration was isolated from the machine base by an air film suspension system which isolated vibrations of 1Hz frequency.

Analysis of errors due to noise

The noise errors in the measurements arise from two main sources: detector "shot" noise and roughness of the scanner slot edges. Shot noise is caused by variation in the rate at which photons hit the photocathode of the detector. The photon input varies randomly as $N^{\frac{1}{2}}$, where N is the statistical mean number of photons per second hitting the photocathode and $N^{\frac{1}{2}}$ is variance of the normal curve centered on N. A photon flow of $N \pm N^{\frac{1}{2}}$ produces an electron flow of $N' \pm N'^{\frac{1}{2}}$ in the photodetector. The rms noise current is usually expressed as

$$i_{\rm N}=(2qBi_{\rm S})^{\frac{1}{2}},$$

where q is the charge of an electron, i_8 is the average detector current and B is the bandwidth of the electronic

646

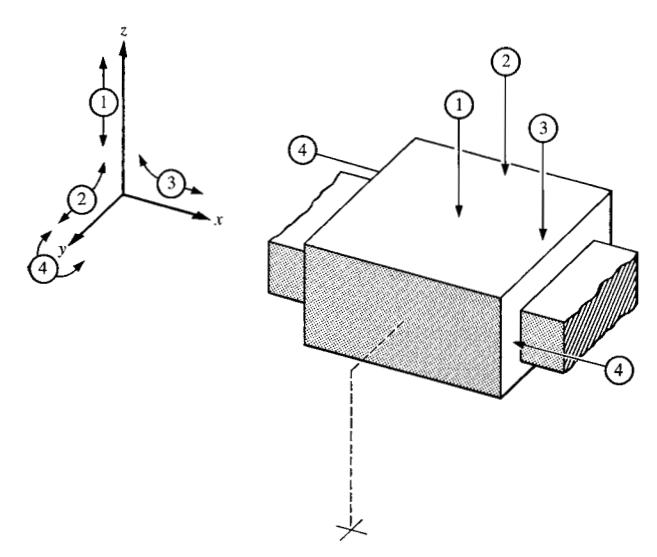


Figure 7 Points on scanner carriage at which force was applied to determine characteristics of machine base.

system. The optimum bandwidth is B=1/T, where T is the time needed for the aperture to move across an edge of a part. The signal-to-noise ratio at the maximum signal level, $i_{\rm S}=I$, and bandwidth B=1/T is

$$(S/N) = (IT/2q)^{\frac{1}{2}}.$$

Any attempt to improve the signal-to-noise ratio by increasing the detector current I and/or by taking a longer time T to make each measurement will require some trade-offs among the speed, resolution and accuracy of the PAMM.

• Measurement error due to detector noise

The error due to photodetector noise can be determined by calculating the width of the "noise band" (see Fig. 9) at the I/2 level of the output signal, i_s . The limits of the noise band can be expressed as a function y(x) defined over the range T:

$$y = i_{S}(x) \pm \frac{1}{2}i_{N}(x),$$

where the choice of plus or minus sign selects the upper or lower limit, respectively. Since the average detector current varies with x as

$$i_{\rm S}=I\left(1-\frac{x}{T}\right),\,$$

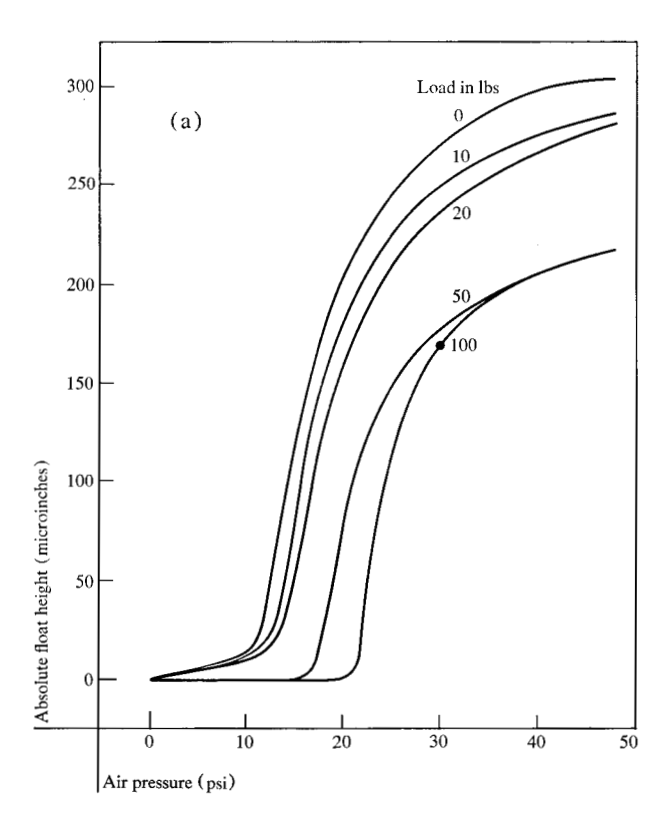
and the rms noise current varies as

$$i_{\rm N} = (2qBi_{\rm S})^{\frac{1}{2}} = (2qBI)^{\frac{1}{2}} \left(1 - \frac{x}{T}\right)^{\frac{1}{2}},$$

the expression for the noise band limits is

$$y = I\left(1 - \frac{x}{T}\right) \pm n\left(1 - \frac{x}{T}\right)^{\frac{1}{2}},$$

where $n = \frac{1}{2}(2qBI)^{\frac{1}{2}}$.



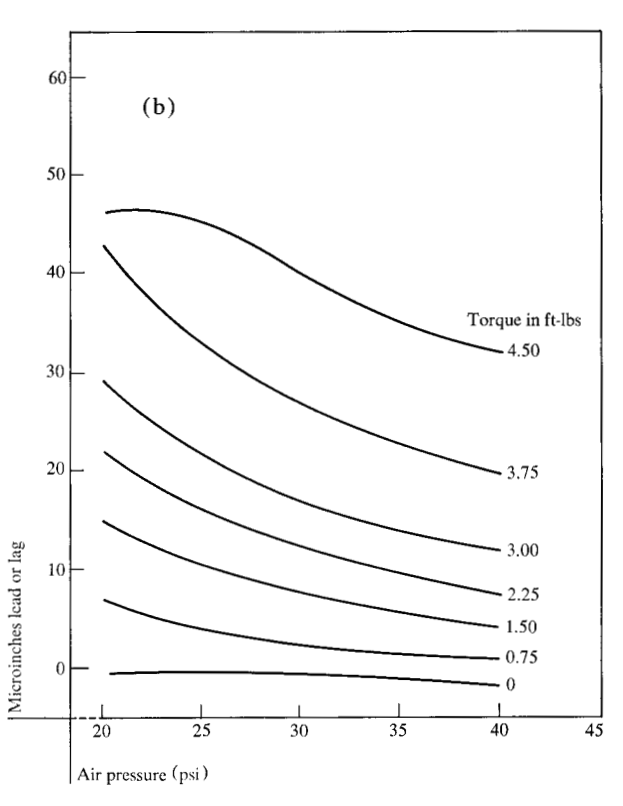


Figure 8 Characteristics of machine base. (a) Float height vs air pressure and load; (b) displacement of optical axis vs air pressure and torque.

647

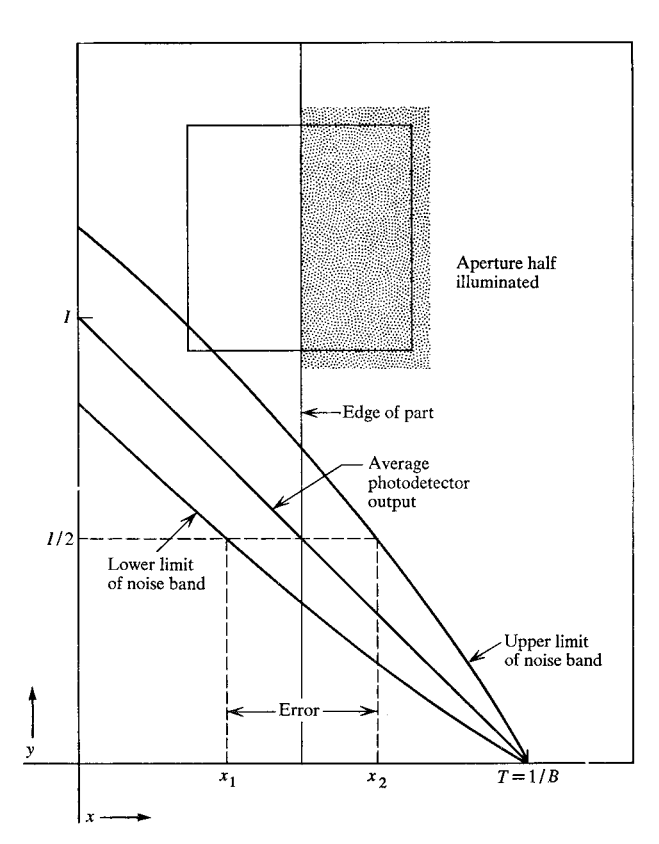


Figure 9 Variation of photodector output and shot-noise band as aperture passes edge of part.

Solving for x at y = I/2 gives the two values, x_1 and x_2 , whose difference is the error in determining the location of a part edge:

$$x_{1,2} = \frac{T}{2} \left[\left(1 - \frac{n^2}{I^2} \right) \pm \left(\frac{n^4}{I^2} + \frac{2n^2}{I^2} \right) \right]^{\frac{1}{2}}.$$

$$E = x_1 - x_2 = T \left(\frac{n^4}{I^4} + \frac{2n^2}{I^2} \right)^{\frac{1}{2}}$$

$$= 2^{\frac{1}{2}} T \frac{n}{I} \left(\frac{n^2}{2I^2} + 1 \right)^{\frac{1}{2}}.$$

Because an expression of the form $(1 + a)^{\frac{1}{2}}$ is approximately equal to 1 + (a/2) for small values of a,

$$E\approx 2^{\frac{1}{2}}T\frac{n}{I}\left(1+\frac{n^2}{4I^2}\right).$$

The possibility for making any measurement requires that n be less than I/2. This means that the term $n^2/4I^2$ must be less than 1/16 and can be ignored. Thus,

$$E \approx 2^{\frac{1}{2}} T \frac{n}{I} = \left(\frac{qT}{I}\right)^{\frac{1}{2}}$$
 seconds.

To convert the error to linear dimensions, E must be multiplied by the scan rate, which was defined earlier

as r = ls/M in./sec, where l is the length of the scan in inches (i.e., difference between maximum and minimum spiral radii), s is the disk speed in revolutions per second and M is the lens magnification. Taking r = 7.5 in./sec., $T = 33 \, \mu \text{sec}$ and $I = 10^{-8}$ as typical values, the calculated error is 1.88×10^{-7} in.

The effects of reducing the aperture area by a factor 1/k are to reduce detector current by a factor $1/k^2$ and to reduce the time required for the aperture to move across the part edge by a factor 1/k. Thus, if T' = T/k and $I' = I/k^2$, the detector error is increased by a factor $k^{\frac{1}{2}}$:

$$E' = \left(\frac{qT'}{I'}\right)^{\frac{1}{2}} = \left(q \frac{T}{k} \frac{k^2}{I}\right)^{\frac{1}{2}} = k^{\frac{1}{2}} E.$$

Increasing the lens magnification by a factor k reduces the detector current by a factor $1/k^2$, and, thus, the linear measurement error is not affected since the two changes cancel each other. If M' = kM and $I' = I/k^2$,

$$E = \left(\frac{qT}{I'}\right)^{\frac{1}{2}} \left(\frac{sl}{M'}\right) = \left(\frac{qTk^2}{I}\right)^{\frac{1}{2}} \left(\frac{sl}{kM}\right) = E.$$

• Noise error due to aperture roughness

The passage of light through an aperture with rough edges results in modulation of the average photodetector current i_8 by a noise signal $i_N = 2^{\frac{1}{2}} \sigma I/D$, where D is average length of the aperture edge, σ is the rms size of the edge roughness and I is the detector current of the fully illuminated aperture. This noise produces an indeterminacy in finding the point where the photodetector current has an amplitude I/2. The expression for the noise band limits (see Fig. 10) as a function y(x) is

$$y = \left(I \pm \frac{\sigma I}{2D}\right)\left(1 - \frac{x}{D}\right),\,$$

where the plus and minus signs refer to the upper and lower limits, respectively. Similar to the calculation of detector noise error, at y = I/2

$$x_{1,2} = D \left[1 - \frac{1}{2(1 \pm \sigma/2^{\frac{1}{2}}D)} \right]$$

and

$$E = x_1 - x_2 = \frac{1}{2^{\frac{1}{2}}} \frac{\sigma}{1 - (\sigma/2^{\frac{1}{2}}D)^2} \approx \frac{\sigma}{2^{\frac{1}{2}}}$$
 inches.

This is the error at the image plane. To calculate the error at the object plane, divide E by the lens magnification M. The value of σ for the disk used in the Precision Automated Measuring Machine is 5 μ in. This gives an error due to edge roughness of 1.77×10^{-7} in.

PAMM computer application

Control of the PAMM is one application currently implemented on the satellite computer system⁷ installed

at the IBM Rochester plant. The satellite computer is an IBM 1130 with a 32K core storage and a storage access speed of 3.6 µsec per 16-bit word.

A specially designed Process Control Unit (PCU) is interfaced to the PAMM and the 1130 (Fig. 11). It provides the circuits and controls necessary to assemble data from the PAMM and transmit it to the 1130 and also controls the PAMM's scanner and table movement.

The PAMM description of the part to the computer is in the form x-y coordinates outlining the part edges and holes. As the part is being scanned and the scan aperture moves across an edge, a signal is sent to the PCU which immediately causes the x-y interferometer counter outputs and the angular position counter to be buffered in the PCU. The angular position counter is located in the PCU and is used to indicate the angular position of the scanning disk or the position of the scan aperture. Twenty-five bits of data are buffered from each interferometer counter and 13 bits from the angular position counter. Since the 1130 operates on a 16-bit word, four words of data are required for each coordinate from the PAMM. The PCU requests a cycle-steal operation from the computer and within 18 µsec transmits the four words to the computer.

The computer program positions the table and scanner so as to place the part and scanner at a predetermined starting position. The x-y interferometer counters are monitored to accomplish this. With the table stopped, the scanner is sent across the x bridge and the first portion of data is gathered from the part. The table is then incremented for a distance the length of the scan line and the scanner is brought back across the part. Scanning is continued in this manner until the part has been completely

The angular position count is converted to a laser fringe count and added to the interferometer count. The x-y fringe counts are then multiplied by a factor which is determined by the index of refraction of air for He-Ne frequency at room temperature, pressure and humidity. The resulting data, now in inches, is sorted. Different methods of sorting are used depending on the part being measured. Calculations are now performed on the data which will determine whether or not the specification tolerances are met. Program output is on the IBM 1132 Line Printer.

The software for part analysis has been developed with the idea to provide a means of reducing the programming effort and time required to measure future parts. To accomplish this a set of subroutines and functions for performing repeated tasks have been written and as the need arises new ones may be added. Details of how each subroutine performs its function are omitted here, but descriptions of the major subroutines and a list of functions are included.

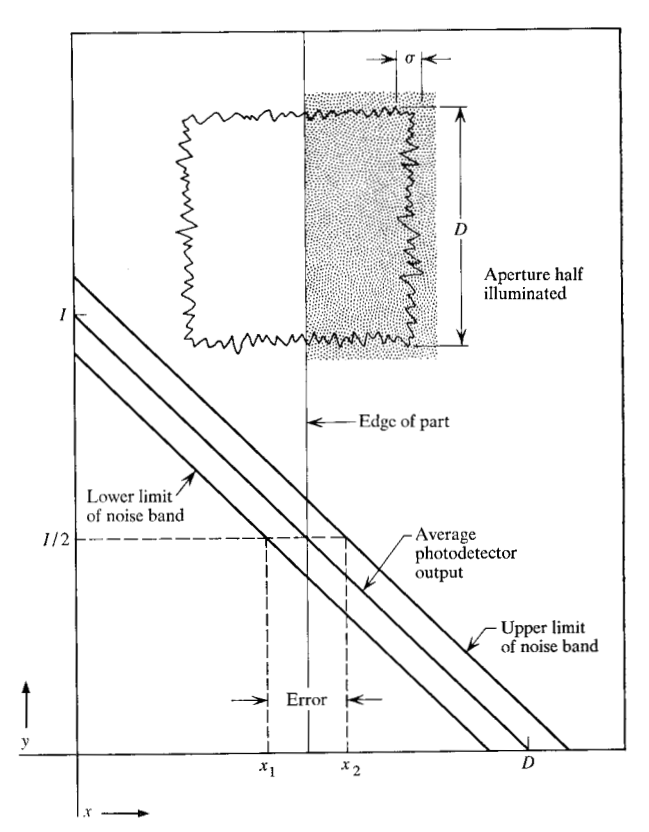
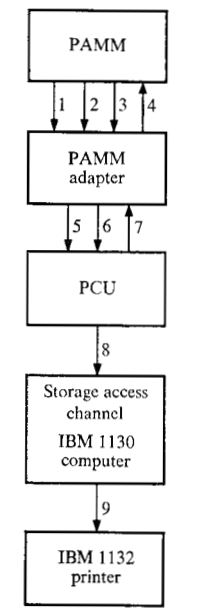


Figure 10 Variation of photodetector output and noise band caused by aperture edge roughness as aperture passes edge

Figure 11 Block diagram of PAMM computer control system.



Signal lines

- Laser interferometer data to bi-directional counters
- Photomultiplier output signals; (a) scanning aperture, (b) angular position and index
- Table and scanner travel limit switches
- Motor control
- Counter outputs
- Table and scanner travel limit switches, and scanning aperture photomultiplier outputs
- Motor control buffer outputs
- Data and timing signals

Measurement results

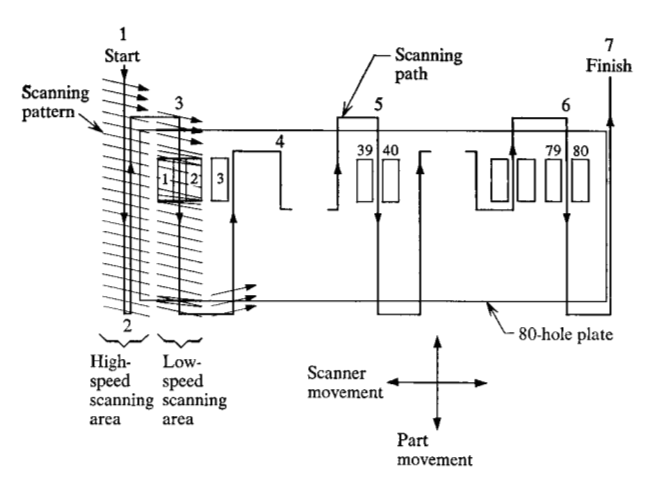


Figure 12 Eighty-hole die plate used for punching cards.

- 1) An edge developing program uses linear regression analysis to fit a straight line through edge data points. It checks for false (such as triggering on a dust particle) data points and then shifts the calculated line to the outermost data point recorded.
- 2) A corner break program checks whether data points are within specified tolerances.
- 3) A corner radius program checks whether data points are within specified tolerances.
- 4) A tolerance program checks whether edge data points are within tolerance from a calculated straight line.

Other geometric information is obtained through the use of function statements to request computation of

- 1) parallelism between lines,
- 2) perpendicularity,
- 3) distance from point to a line,
- 4) distance between two points,
- 5) distance between lines, and
- 6) angles between lines.

The first part to be measured using PAMM is the 80-hole die plate used for punching cards in the IBM 2520 Reader Punch. Figure 12 shows a diagram of the part. To start, the scanner is moved to position 1. As the part is moved beneath the scanner, the first edge is detected and data points are recorded (scanner now located at position 2). During movement to position 3 the first edge is located and corresponding data is stored. Specific data points are deleted unless needed later in the program. From position 3 the part is moved in a similar manner as before. This time the locations of the upper edge, the first two holes and lower edge are recorded. The two outer edge measurements are stored until enough data have been collected for edge analysis. Straight lines

and corner break data points are separated and respective analyses are conducted. Information to be used later, such as hole-alignment data, is stored. Other measurement information concerning whether the specific parts of a hole meet specifications and their actual dimensions are recorded for future print-out. The scanner is now moved to position 4 where a repeated scan and analysis of pairs of holes are made. At holes 39 and 40 (position 5) another scan of the outer edges is made and data are recorded. Continued scans are made until holes 79 and 80 (position 6) are reached, and then outer edges are again scanned. On reaching position 7 the last outside edge is scanned. The overall size of the plate, the distance from first edge to first hole, alignment of holes and distance from holes to upper edge are analyzed. A printout of the actual dimensions for each hole and other required measurements is made. A summary printout shows the dimensions that do not meet specifications.

Appendix A-Michelson interferometer

A simple explanation of the Michelson interferometer shown in Fig. A1 will show how it can be used for measuring purposes. The output beam from the laser is split into two beams by the beam splitter. One beam goes to the fixed mirror M_1 and returns to the beam splitter. Its total path length traveled is L_1 . The other beam from the beam splitter travels to the movable mirror M_2 and returns. Its total path length is L_2 . The two beams are brought back together at the beam splitter and mixed. The mixed beam is directed to the photodetector.

The beam which strikes mirror M_1 travels a total distance of L_1/λ wavelengths. The beam to mirror M_2 travels a total distance of L_2/λ wavelengths. When the two beams mix at the beam splitter they differ in phase by $(2\pi/\lambda)(L_1-L_2)$ radians. When the two waves are in phase or differ by an even multiple of π radians their amplitudes add to produce a maximum and when they are out of phase by any odd multiple of π radians their amplitudes subtract and a minimum results. Since the difference in phase between the two beams is controlled by the position of the movable mirror, any movement can be monitored by recording the number of maxima reaching the photodetector. The expression for the total amplitude at the detector is:

$$A_{\text{total}} = A_1 \sin \omega t + A_2 \sin \left[\omega t + (2\pi/\lambda)(L_2 - L_1)\right],$$

where A_1 and A_2 are the amplitudes of the beams from M_1 and M_2 , respectively, and ω is the frequency of the laser light, $\approx 3 \times 10^{15}$ radians/second. This expression disregards all constant phase shifts and all phase shifts common to both beams due to the optics such as the beam splitters.

The current from the photodetector is proportional to the square of the total amplitude. Also the photo-

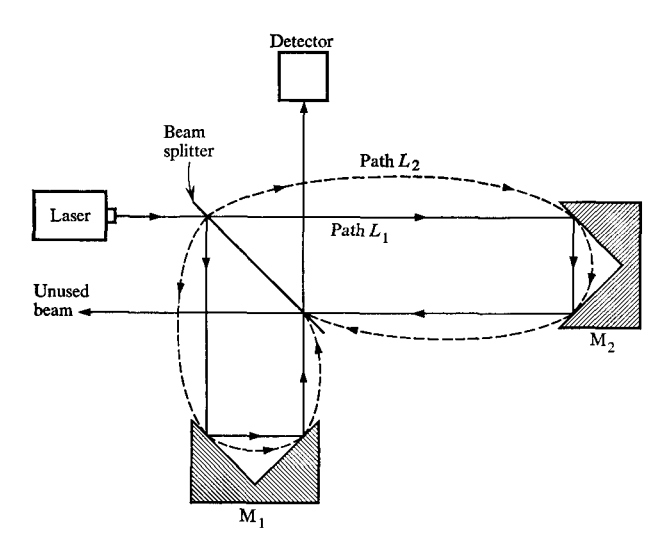


Figure A1 Simple Michelson interferometer.

detector averages the light frequency ω because of its limited response time. The photocurrent is therefore:

$$I = K[1 + \cos(2\pi/\lambda)(L_2 - L_1)]$$

= $2K\cos^2(\pi/\lambda)(L_2 - L_1)$,

where K is a constant determined by the system.

When the movable mirror is moved a distance x, the path length L_2 is changed by 2x. Also, if L_1 is to be an integral number of wavelengths, the expression for the photocurrent can be written as

$$I = 2K \cos^2 [(2\pi x/\lambda) + m\pi]$$
$$= 2K \cos^2 2\pi x/\lambda.$$

The interferometer shown in Fig. A2 has two outputs so that the direction of movement can be monitored. One output I_1 is identical to I above. The quarter-wave plate introduces a phase shift of $\pi/4$ radians in the amplitude of the second output. The expression for the photocurrent I_2 is

$$I_2 = 2K \cos^2 (2\pi x/\lambda + \pi/8).$$

When the movable mirror M_2 moves to the right, the phase of I_1 lags that of I_2 , but when the movable mirror moves left the phase of I_1 leads that of I_2 . In this manner the direction of movement can be monitored and recorded.

The output of the interferometer is a cosine squared waveform with a period of about 12 microinches. This

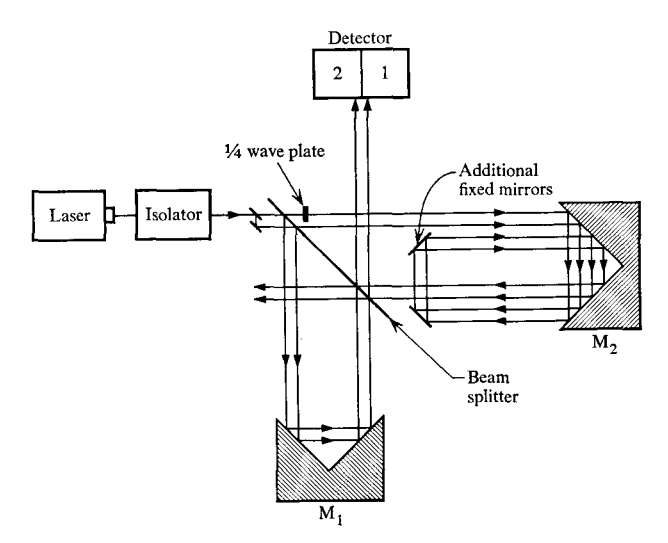


Figure A2 Single-axis double-path Michelson interferometer.

waveform can be electronically subdivided to give a smaller least count. A smaller least count can also be achieved by using a double path system as shown in Fig. A2. As can be seen from the Figure, when the movable mirror is moved a distance x the total path length is changed by 4x. Therefore, when the mirror is moved one-quarter wavelength the total path length is changed by one wavelength, thus producing a full cycle at the detector.

Acknowledgments

The authors acknowledge with gratitude the contributions of C. Geisinger, who developed the disk-slot scanning principle; W. Leary and C. Markley who assisted in developing the original optical parameters.

References

- 1. H. Mote, "Coordinate Measuring Machines," American Machinist Special Report No. 613, January 1, 1968.
- 2. DIG System, Bausch & Lomb Application Brochure.
- 3. Inductosyn Principles and Applications, Farrand Controls, Inc., 99 Wall Street, Valhalla, New York.
- 4. G. Oster and Y. Highhijima, "Moiré Patterns," Scientific American 208, No. 5, 54 (1963).
- 5. Y. Totsuka, "Measure to Microns with Moiré Fringes," Tool & Manufacturing Engineer 61, No. 2, 20 (1968).
- A. L. Bloom, Gas Lasers, John Wiley & Sons, Inc., New York, 1968, p. 89.
- J. E. Stuehler, "An Integrated Manufacturing System: Implementation in IBM Manufacturing," IBM J. Res. Develop. 14, 605 (1970), this issue.

Received January 12, 1970